



HAL
open science

FastEMD–CCA algorithm for unsupervised and fast removal of eyeblink artifacts from electroencephalogram

Ashvaany Egambaram, Nasreen Badruddin, Vijanth S. Asirvadam, Tahamina Begum, Eric Fauvet, Christophe Stolz

► To cite this version:

Ashvaany Egambaram, Nasreen Badruddin, Vijanth S. Asirvadam, Tahamina Begum, Eric Fauvet, et al.. FastEMD–CCA algorithm for unsupervised and fast removal of eyeblink artifacts from electroencephalogram. Biomedical Signal Processing and Control, 2020, 57, pp.101692 -. 10.1016/j.bspc.2019.101692 . hal-03489122

HAL Id: hal-03489122

<https://hal.science/hal-03489122>

Submitted on 21 Jul 2022

HAL is a multi-disciplinary open access archive for the deposit and dissemination of scientific research documents, whether they are published or not. The documents may come from teaching and research institutions in France or abroad, or from public or private research centers.

L'archive ouverte pluridisciplinaire **HAL**, est destinée au dépôt et à la diffusion de documents scientifiques de niveau recherche, publiés ou non, émanant des établissements d'enseignement et de recherche français ou étrangers, des laboratoires publics ou privés.



Distributed under a Creative Commons Attribution - NonCommercial 4.0 International License

FastEMD–CCA Algorithm for Unsupervised and Fast Removal of Eyeblink Artifacts from Electroencephalogram

Ashvaany Egambaram^{a,c,e}, Nasreen Badruddin^{a,c}, Vijanth S Asirvadam^{b,c}, Tahamina Begum^d, Eric Fauvet^e, Christophe Stolz^e

^a*Institute of Health and Analytics, Universiti Teknologi PETRONAS, Perak, Malaysia*

^b*Institute of Autonomous Systems, Universiti Teknologi PETRONAS, Perak, Malaysia*

^c*Department of Electrical and Electronic Engineering, Universiti Teknologi PETRONAS, Perak, Malaysia*

^d*Department of Neuroscience, Universiti Sains Malaysia, Kelantan, Malaysia*

^e*Laboratoire Electronique, Informatique et Image (Le2i), ERL VIBOT CNRS 6000, Universite de Bourgogne, France*

Abstract

Online detection and removal of eye blink (EB) artifacts from electroencephalogram (EEG) would be very useful in medical diagnosis and Brain-Computer Interface (BCI). In this work, approaches that combine unsupervised eyeblink artifact detection with Empirical Mode Decomposition (EMD), and Canonical Correlation Analysis (CCA), is proposed to automatically identify eyeblink artifacts and remove them in an online manner. First eyeblink artifact regions are automatically identified and an eyeblink artifact template is extracted via EMD, which incorporates an alternate interpolation technique, the Akima spline interpolation. The removal of eyeblink artifact components relies on the elimination of EEG canonical components obtained through CCA, based on cross-correlation with the extracted eyeblink artifact template. The proposed algorithm is evaluated and analysed with respect to its ability in removing eyeblink artifacts and retaining neural information of the EEG signals. Analysis proved that the proposed algorithm, FastEMD-CCA, is effective in eyeblink ar-

Email addresses: ashvaany_g03337@utp.edu.my (Ashvaany Egambaram), nasreen.b@utp.edu.my (Nasreen Badruddin), vijanth_sagayan@utp.edu.my (Vijanth S Asirvadam), tahamina@usm.my (Tahamina Begum), eric.fauvet@u-bourgogne.fr (Eric Fauvet), christophe.stolz@u-bourgogne.fr (Christophe Stolz)

tifact removal with an average accuracy, sensitivity, specificity and error rate of 97.9%, 97.65%, 99.22% and 2.1% respectively. The algorithm is able to clean and remove eyeblink artifacts from a 14-channel EEG of length 1 second, at an average time of 63 milliseconds. This makes it a feasible solution for applications requiring online removal of eyeblink artifacts.

Keywords: Electroencephalogram (EEG), Enhanced Empirical Mode Decomposition (FastEMD), Canonical Correlation Analysis (CCA), Eyeblink Artifact.

1. Introduction

An electroencephalogram (EEG) is used to record and evaluate electrical potentials generated during cerebral activity. The EEG signal has been in use to interpret cognitive processes and physiological activity of the brain for medical purposes and extensively used for various research purposes. An EEG signal does not only consist of electrical potentials related to brain activities, but it is invariably contaminated by electrical signals originating from other parts of the body. These unwanted signals are referred to as artifacts. The superimposition of these artifacts with the EEG signal could potentially lead to inaccurate EEG interpretation. This issue is particularly relevant in the medical field where EEG signals are widely used as a diagnostic tool, thus failing to recognize and remove artifacts may affect clinical decisions. Therefore, artifact identification and removal in EEG signal processing are the first and most crucial step.

The most common types of artifacts contaminating EEG signals are the cardiac artifact, the muscle artifact and the eye blink artifact [1]. The muscle artifact is caused by muscle movement and contraction, which may take place when the patient talks or swallows. The cardiac artifact solely arises from the electrical activity of the heart. Out of all these artifacts, eyeblink artifact is the one most prominently present in EEG signals as blinking the eyes produces relatively large electrical potentials around the eyes, hence this work will focus on identifying and removing it. Eyeblink artifacts appear as spikes with am-

plitudes of around 10 times greater than the actual brain signals, noticeable in the delta wave range and can last up to 200ms to 400ms [2, 3]. The eyeblink potential propagates and spreads out to all EEG electrodes but in various conduction volume - higher conduction near the frontal and parietal regions while the conduction in the occipital region is very low. The frontal region is the most prone region to contamination from eyeblink artifacts as it is closest to the eyes. Fig. 1 shows the positions of EEG electrodes following the 10-20 system. The Fp1 and Fp2 electrode positions, which are closest to the eyes and highlighted in Fig. 1, can be used to capture the eyeblink artifacts.

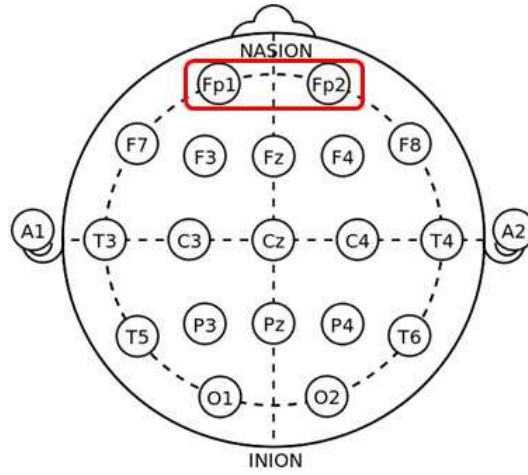


Fig. 1: EEG Electrode Placement

For reliable analysis of EEG signals, it is therefore essential that these artifacts be removed. Traditionally artifact removal is done after the EEG signal has been recorded, either manually or automatically. However, in clinical monitoring such as continuous epilepsy monitoring and the brain-computer interface (BCI), where EEG signals are analyzed and manipulated as they are being recorded, an online artifact removal solution is required [4]. Various techniques are available for de-noising purposes, which will be discussed below. The most common method is to have eyeblink artifact regions identified through manual inspection and these segments are removed. This method can cause a loss

of information as the EEG segments being removed may contain useful neurological information. Regression-based methods [5–7] perform a regression or correlation test between the signal to be processed and a reference signal. For example, electrooculogram (EOG) signal can be used as the reference signal to be compared with the EEG signal. The segment of the EEG signal that highly correlates with the EOG is then assumed to be related to the eyeblink artifacts and thus removed. However, since EOG also contains some EEG potentials due to the close proximity of EOG electrodes to the frontal region of the brain, artifact removal via regression methods may also remove important EEG data. In addition, a reference electrode is obligatory in regression-based methods, which may cause discomfort to patients when there is an extra pair of electrodes placed around the eyes especially for longer EEG recordings.

In [8], Principal Component Analysis (PCA) is used to isolate out components of the highest variance between EOG and EEG signals. The highest variance components are the principal components and are classified as eyeblink components. Similar to regression-based methods, PCA also requires additional EOG electrodes to be applied. Besides that, it is not able to completely separate some artifacts from the raw EEG signal in the event that both the eyeblink and EEG signals have comparable amplitudes [9]. On the other hand, Independent Component Analysis (ICA) [10, 11] is proven to be able to remove eyeblink artifacts, as well as artifacts from different sources, but it may not be suitable for online applications as visual inspection on the independent components (ICs) is required to manually identify and select ICs corresponding to artifacts [12]. To overcome this, some work has been done to automate artifact detection and removal by combining ICA with other methods like Wavelet or Empirical Mode Decomposition. However, in all these cases the computational complexity stands out as a limiting factor for ICA to be used in online applications [13]. The Wavelet transforms on the other hand depends on choosing a suitable decomposition mother wavelet. The mother wavelet is a function comprising sine and cosine waves, thus most of the time it will not characterize or adapt to non-linear EEG signals, producing decomposition errors [12].

Canonical Correlation Analysis (CCA) [14], has been used in muscle and eyeblink artifact removal and has been proven to be the fastest among other de-noising techniques discussed above [15]. However, if CCA is to be used alone to remove artifacts, it still requires an additional reference signal to identify the artifact events. Instead of using a reference signal, Empirical Mode Decomposition (EMD) can be used to extract the eyeblink artifact signal from the EEG signal [15–18]. EMD [19] is an algorithm that decomposes a signal without requiring any pre-knowledge or pattern of interest, unlike other de-noising techniques. In a comparative study on extracting out a biomedical signal [20], EMD is proven to be more accurate compared to the wavelet transform. On top of that, a method combining EMD and CCA (EMD-CCA) in [15], is shown to outperform CCA, FastICA and EMD-FastICA in terms of artifact removal accuracy, when evaluated on an EEG signal added with a synthetically generated eyeblink artifact. Despite the fact that it can accurately remove artifacts from the EEG signal compared to other techniques, the algorithm is relatively slow due to its iterative nature.

Most of the techniques on eyeblink artifact removal discussed above are used only for offline artifact removal. Since applications such as BCI and epilepsy monitoring require online signal processing, artifact removal methods and algorithms should be capable of online processing. Hence, to cater to online artifact removal, the methods or algorithm should satisfy a few criteria. The most important requirement is that the algorithm should be fully automatic without any expert’s intervention. Secondly, online applications should avoid utilizing additional electrodes around the artifact originating regions, such as EOG, as it may cause discomfort and inconvenience to the subject during long-term EEG recordings. Finally, online implementation requires the artifact removal algorithm to have minimal computational complexity so that the algorithm doesn’t introduce an unacceptable time delay.

Researchers have studied hybrid techniques to detect and remove eyeblink artifact from EEG signal which may be useful for online applications [21–23]. Some of these techniques are discussed here. Lawhern et al. in [24] used the

Auto-regressive (AR) model for artifact feature selection followed by a Support Vector Machine (SVM) classifier for training purposes to detect the artifacts. Nguyen et al. [25], have reported their work on ocular artifact removal by combining Wavelets and Artificial Neural Network (ANN), and naming their technique Wavelet Neural Network (WNN). This technique requires an EOG reference channel to train the ANN classifier. Zhao et al. [13] used Discrete Wavelet Transformation (DWT) and an Adaptive Predictor Filter (APF) to remove ocular artifacts from EEG signals. Daly et al. [26] have developed a software plugin GUI, called the Fully Online and Automated Artifact Removal for Brain-Computer Interfacing (FORCe). This plugin works based on the combination of Wavelet Decomposition, Independent Component Analysis and thresholding. FORCe runs in MATLAB and it is stated that it can be used for online BCI applications, making it the only software plugin that is able to perform significantly faster. Most recently, Tonachini et al. in [27] has developed an online automatic artifact rejection using artifact subspace reconstruction (ASR), online recursive independent component analysis (ORICA) and an IC classifier. However, the author has stated that ASR had negligible effect on eyeblink artifact removal, and the time it took for ORICA to converge well enough on the blink-related IC for the artifact to be removed is 26 seconds, which is a significant amount of time.

To the extent of the authors' knowledge, every online artifact removal technique discussed above depends on either a dedicated artifact reference recording or some kind of training data that records artifacts separately for training purposes, which may add some time delay to the techniques in online applications. This work first focuses on introducing a novel unsupervised eyeblink artifact detection algorithm which identifies eyeblink artifact regions effectively, assisting subsequent artifact removal process. Secondly, the performance of EMD is improved with various enhancements to resolve the processing time inefficiency of the algorithm. Next, the enhanced version of EMD is applied on the most relevant eyeblink artifact region identified through the unsupervised artifact detection algorithm to extract out a suitable eyeblink artifact template. Finally,

our work makes use of the artifact template extracted as a reference in identifying subsequent eyeblink artifacts instead of relying on an EOG recording. With the help of the artifact template, the identified eyeblink artifact regions are subjected to CCA for eyeblink artifact removal in online applications. The direction of the work is to provide an application-centric solution for online applications with reasonable/reduced complexity and enhanced performance. The developed algorithm neither depends on a separate EOG recording or an expert's advice for eyeblink events identification, thus removing any constraints in terms of automation for online implementation. Additionally, no training data is required beforehand for the algorithm to learn and identify eyeblink artifacts. The developed algorithm is compared with one of the state-of-the-art methods, i.e. FORCe, due to its effectiveness in removing eyeblink artifacts and its low computation time. The next section elaborates the proposed algorithm and the materials used in this work, while results and discussions are presented in Section 3. Finally, we conclude the paper with some recommendations in Section 4.

2. Materials and Methods

2.1. *Unsupervised Eyeblink Artifact Region Detection*

Since the frontal region of the brain is the nearest region to the position of eyes, eyeblink artifacts can be easily captured in this region, so the Fp1 and Fp2 electrodes should hypothetically exhibit high correlation whenever there is an occurrence of an eyeblink. To validate this theory, the correlation coefficient is computed between Fp1 and Fp2 in windows of 500 samples (1.95 seconds). As eyeblink artifacts can last up to 800ms [2, 3], this window size will allow at least one eyeblink artifact to fall within the window. The test has revealed that segments of Fp1 and Fp2 without eyeblink artifact produce correlation below than 0.7, whereas segments containing eyeblink artifact results in higher correlation, usually more than 0.9 as illustrated in [28] and shown in Fig. 2.

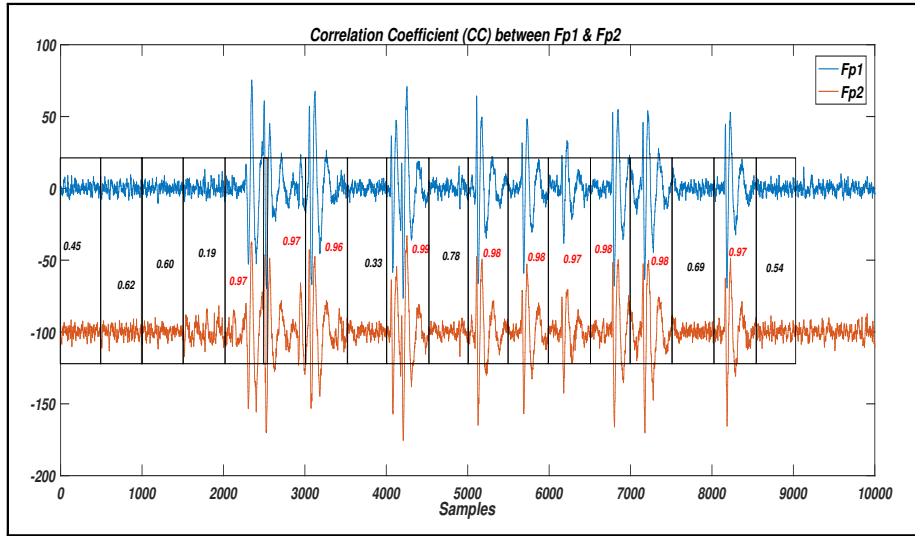


Fig. 2: Correlation Coefficient, CC, between Fp1 and Fp2 Electrodes

In order to design an automatic eyeblink artifact region detection algorithm, first a high value of correlation coefficient that is greater than 0.85 is set to indicate the presence of an eyeblink artifact in that particular window. However, the eyeblink potentials and starting point of the eyeblink artifact should be identified for subsequent analysis or artifact removal, which requires a threshold. The displacement of amplitude is chosen as the threshold criterion as eyeblink artifacts are in general, higher in amplitude relative to that of the EEG or brain signal. Therefore, the eyeblink artifact components are expected to produce higher amplitude displacement compared to uncontaminated EEG potentials. First, the amplitude displacement from the mean is calculated within an Fp1 window that exhibits a high correlation with Fp2. The displacement distribution from the mean amplitude is computed using Eq. (1):

$$\text{Displacement}[t] = |X[t] - \mu| \quad (1)$$

where, $X[t]$ is the EEG signal's amplitude at time t , and for any given window starting at sample point n , $X[t]$ is evaluated from $t = n$ to $t = n + 500$, and μ

is the mean of that particular window.

An experiment conducted by the authors in [28] has shown that the threshold for eyeblink artifact's onset point and eyeblink potentials dominating the EEG window in question can be correctly determined by taking two standard deviation, 2σ width from the mean of the displacement distribution acquired, as in Eq. (2). Any absolute value beyond 2σ is classified as an eyeblink artifact potential and the first sample that exceeds this threshold is considered as the eyeblink artifact's starting point.

$$\text{threshold} = \text{mean} + 2\sigma \quad (2)$$

Later, the onset of eyeblink artifact is moved 100 samples (0.39 seconds) ahead. The reason for setting the onset point in advanced of 100 samples before the threshold is to provide a buffer for any subsequent analysis. The end point of the eyeblink artifact is then set to 256 samples, or 1 second, after the first sample with an amplitude displacement crossing the threshold. The eyeblink artifact region is therefore taken to be from the onset of eyeblink till the end point of the eyeblink. Thus, an eyeblink which can last up to 0.8 seconds (205 samples) in duration completely fit into this window (100+256=356 samples).

Several eyeblink artifact regions are searched and saved in a similar way until any two eyeblink artifact regions exhibit correlation coefficient of more than 0.9 between them. The correlation coefficient value of more than 0.9 is chosen assuming that a high correlation between the eyeblink artifact regions denotes repetitiveness or similarity in the blinking pattern of an individual. Hence these regions with high similarity or correlation will be subjected for further analysis, which is the EMD algorithm in this research work. Fig. 3 summarizes the algorithm in a flowchart. Fig. 4 shows the plot of a real EEG signal's eyeblink artifact regions identified through the proposed eyeblink artifact detection algorithm located on the Fp1 channel.

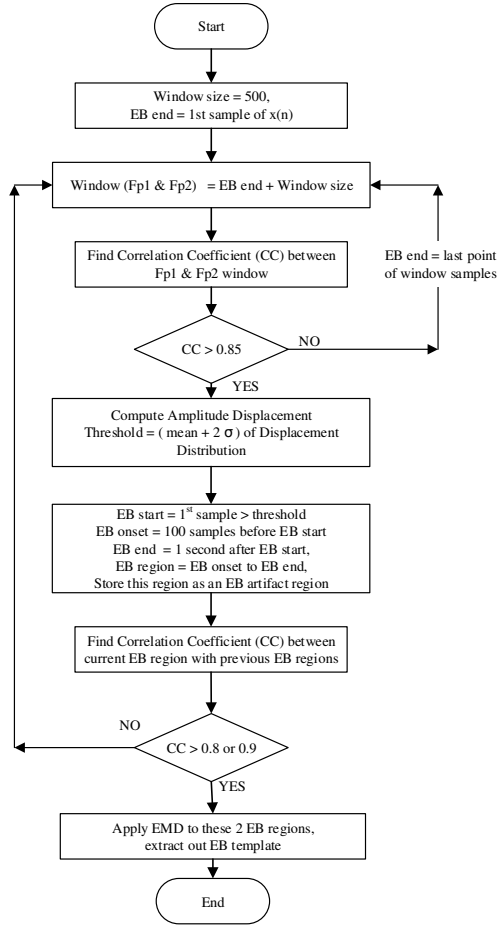


Fig. 3: Flowchart of the Automated Eyblink Region Identification Algorithm

2.2. Eyblink Artifact Template Extraction Through Enhanced EMD (FastEMD)

2.2.1. Introduction to Empirical Mode Decomposition (EMD)

Empirical Mode Decomposition (EMD) is an algorithm that decomposes a signal into multiple oscillating components. The algorithm reiterates itself until it can isolate the highest oscillating component that remains in a signal. This is achieved by identifying relative extrema (maximum/minimum) points in a signal, followed by forming upper/lower envelopes by interpolating these points and removing the mean of the envelopes from the signal. This process is called "sifting", where it continually sifts out a local high oscillating trend

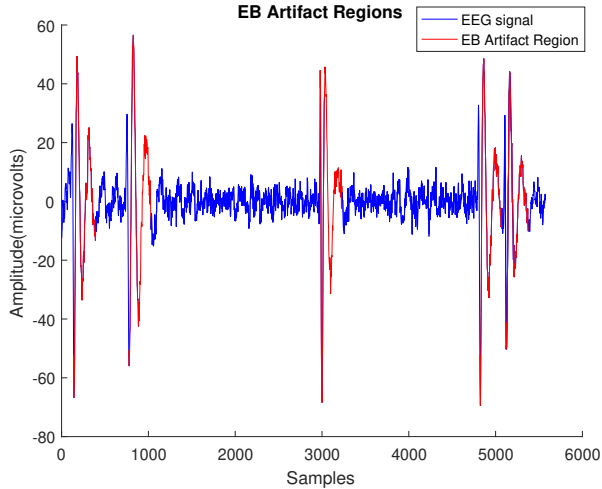


Fig. 4: Eyeblink Artifact Regions Identified through Proposed Method

called the Intrinsic Mode Functions (IMF). Each IMF extracted out from the original signal is a lower oscillating trend compared to its predecessor. Adding up all IMFs and the remaining residual signal obtained from the decomposition would reconstruct the original signal. Each IMF should satisfy the following criteria as in [19]:

- contains an equal number of extrema and zero crossings, or differ at most by one
- envelopes of the IMF are symmetric with respect to zero

In general, $X(t)$ is decomposed into multiple oscillating components called IMFs, $x_i(t)$ and a residual component, $R_n(t)$ which is monotonous, as in Eq. (3):

$$X(t) = \sum_{i=1}^{n-1} x_i(t) + R_n(t) \quad (3)$$

Each sifting loop produces the i -th IMF of the algorithm, $x_i(t)$. The recursive sifting discontinues after the algorithm extracts out $n - 1$ IMFs, the instance

where the residual signal, $R_n(t)$ becomes a monotonic trend. The algorithm is relatively slow because it reiterates itself until the final residual signal becomes a monotonic function.

2.2.2. Proposed Approaches: Enhanced Empirical Mode Decomposition (FastEMD)

EMD is enhanced to resolve the processing time inefficiency of the algorithm through approaches discussed in the following subsections.

Envelope Interpolation in EMD

The performance of EMD algorithm through alternative interpolation techniques is discussed in this section. A major concern in EMD's sifting process relies on how the upper and lower envelopes are being constructed through interpolation. In online applications, EMD could cause the overall processing time to increase as the algorithm is iterative and dependent on interpolating large number of extrema. The interpolation involved would directly consume a lot of the computer resources, hence EMD can be inefficient while removing eyeblink artifacts from lengthy EEG signals, especially in online processing.

As to enhance the performance of EMD algorithm, other interpolation techniques were tested and evaluated in another work. Among alternative interpolation techniques investigated are the Cubic Hermite Spline Interpolation (CHSI) and the Akima Spline Interpolation (ASI). These two interpolation techniques were investigated in terms of their ability to retain the reconstruction accuracy after decomposition and their speed compared to Cubic spline interpolation (CSI), that is used in the classical EMD algorithm. The ASI has produced the highest correlation coefficient of 0.9063, lowest Root Mean Square Error (RMSE) of 3.3, lowest percentage root means square difference (PRD) of 44%, better Signal to Noise Ratio (SNR) of 8.5dB and faster computation time of 0.24s, in decomposing an artificial EEG signal compared to CSI. These results justify that the ASI technique serves a lower computational burden to EMD algorithm with higher reconstruction accuracy and shorter computation time as shown in [29]. Envelope construction through CSI fulfil second-order derivation

at every extremum point to ensure continuity and spline curvature smoothness. Since envelope construction through CSI force two adjacent splines to be continuous at first and second derivatives, the formed envelopes are susceptible to overshoots and undershoots. This produces an erroneous mean estimation during sifting and this error could eventually get transferred and added to the whole data set on every iteration of EMD's sifting process, resulting in an inaccurate and unreliable decomposition. While the envelope construction of ASI depends only on the slopes of adjacent segments with continuity up to first order derivative. Although ASI produces envelopes that are not as smooth as the CSI does, but it demonstrates a better decomposition accuracy. This also reduces the necessity to solve large system equations which in turn, reduces the computation time.

Fixed Number of IMFs

Another factor that limits EMD in online applications is the repetitive sifting process required in obtaining the IMFs. Sifting in EMD algorithm can be classified as redundant in two aspects. First, the algorithm has to repeat sifting plenty of times before any of the resulting trend satisfies the IMF criteria, and thus can be classified as an IMF. Secondly, the algorithm has to reiterate itself multiple times to attain multiple numbers of such IMFs, because it can't terminate sifting until the residual signal becomes a monotonous function. Therefore, IMF extraction through repetitive sifting iterations causes EMD algorithm to be computationally inefficient and slow.

To overcome this issue, the number of IMFs extracted out through EMD is fixed to a constant number. The higher oscillations in the raw EEG signal will be isolated out in the first or second IMFs, hence the sum of remaining IMFs would by default produce an eyeblink artifact trend. Hence, by partially reconstructing the higher oscillating trends which are lower in amplitude would yield the EEG trend. Alternatively, low oscillating trends with high amplitudes are summed together to attain the eyeblink artifact trend. Therefore, EMD's algorithm is re-designed to decompose the raw EEG signal up to 5 to 8 IMFs,

which is sufficient to segregate out the EEG trend and the eyeblink trend.

$$X_{\text{EEG}}(t) = \sum_{i=1}^2 x_i(t) \quad (4)$$

$$X_{\text{eyeblink}}(t) = \sum_{i=3}^5 x_i(t) + R_6(t) \quad (5)$$

This automatically reduces the computation time and the algorithm does not have to repeat itself until a monotonic residue is acquired. The eyeblink artifact template obtained by adding up the 3rd IMF onwards with the residual signal is shown in Fig. 5.

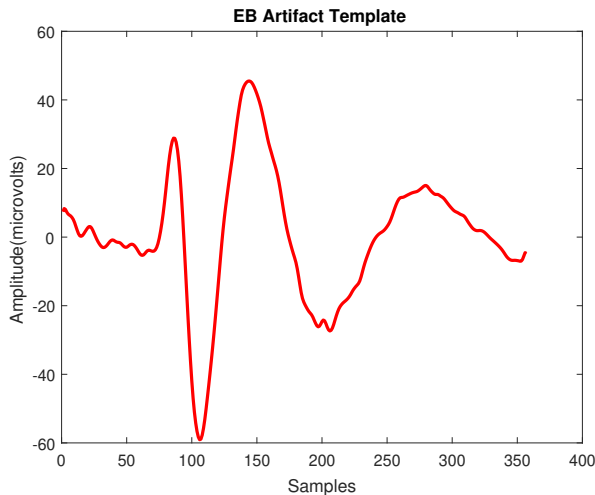


Fig. 5: Extracted Eyeblink Artifact Template

Optimal Use of EMD in Eyeblink Artifact Template Extraction

In applications that require online monitoring of EEG signals, the applications could not wait until the entire EEG signal is recorded for analysis, it may take from few hours to days for an EEG recording to be completed. The eyeblink artifacts have to be removed instantaneously from the EEG recording as well. EMD algorithm is not recommended to be applied after the recording is complete, as it may cause a delay in interpreting an EEG signal and applying EMD on the entire EEG recording will cause the application to get computationally

heavy. As an option, EMD can be applied repetitively on short segments, whenever an eyeblink artifact event is captured, provided the occurrence of eyeblinks are known. Unfortunately, EMD gets computationally inefficient and slow on repetitive application to a huge dataset especially during online recording and analysis, which may even disrupt the recording task.

To resolve this, two eyeblink regions identified in section 2.1 with cross-correlation of more than 0.9, indicated with boxes in Fig. 6 are subjected to EMD separately. EMD is applied only on two most correlating eyeblink artifact regions, thus keeping the number of EMD applications lowest as possible. These two eyeblink regions are chosen as these regions are repetitive in terms of the blinking pattern, which can be assumed as a general eye blinking pattern for that particular EEG signal. This prevents EMD to be used repetitively, especially when the EEG signal is processed in an online manner. This method is different compared to what is being practised in classical artifact removal technique through EMD, where EMD will be applied to remove the artifacts whenever an artifact event is identified. The low oscillating IMFs obtained through EMD are then added, as in Eq. (5), and averaged out to get an eyeblink artifact template.

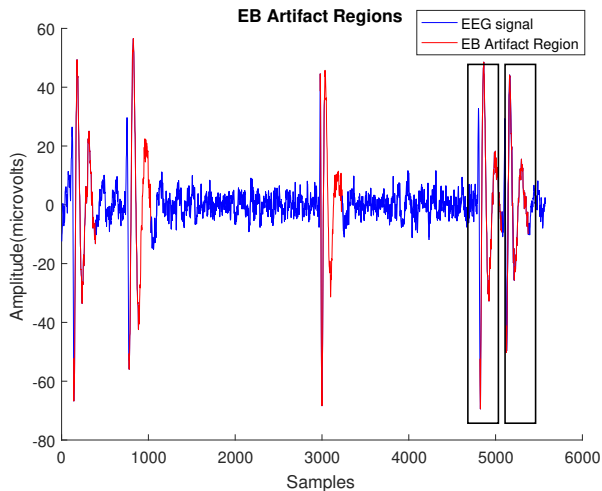


Fig. 6: Highly Correlating Eyeblink Artifact Regions Subjected to EMD

Stopping Criterion for EMD

The work also adopts a stopping criterion for EMD based on the standard deviation which was introduced in [19]. The standard deviation (SD) is defined as the normalized squared difference between two sifting iterations, which is assumed to indicate consistency between two sifting outputs. The SD value calculated from two consecutive sifting outputs, $y_j(t)$ and $y_{j-1}(t)$ should be less than a pre-determined value, normally 0.2 or 0.3 to stop the sifting iteration in EMD.

$$\text{SD} = \sum_{t=0}^k \left[\frac{|y_{j-1}(t) - y_j(t)|^2}{y_{j-1}^2(t)} \right] \leq 0.2 \quad (6)$$

where k is the number of samples in the original signal, $X(t)$.

An updated flowchart of EMD with enhancements discussed above is shown in Fig. 7.

2.3. Eyeblink Artifact Removal

2.3.1. Introduction to Canonical Correlation Analysis (CCA)

Canonical Correlation Analysis (CCA), utilizes blind source separation (BSS) technique. As suggested by the name, BSS separates a set of source signals from a set of mixed signals without any priori knowledge about the source signals or the weighted mixing components. The linear relationship between two multidimensional variables is measured. CCA extracts out two sets of source vectors, where the projections of the two multidimensional variables onto extracted source vectors are maximally correlated.

The application of CCA in the EEG signal is elaborated in this section. The observed EEG signal, $x(t)$ is classified as the first multidimensional variable, while the second multidimensional variable is obtained by taking a temporally delayed component of the original observed EEG signal, $y(t) = x(t - 1)$. As the BSS implies the observed EEG signal $x(t)$ is a result of weighted mixing W with clean EEG source signal, $S(t)$:

$$x(t) = WS(t) \quad (7)$$

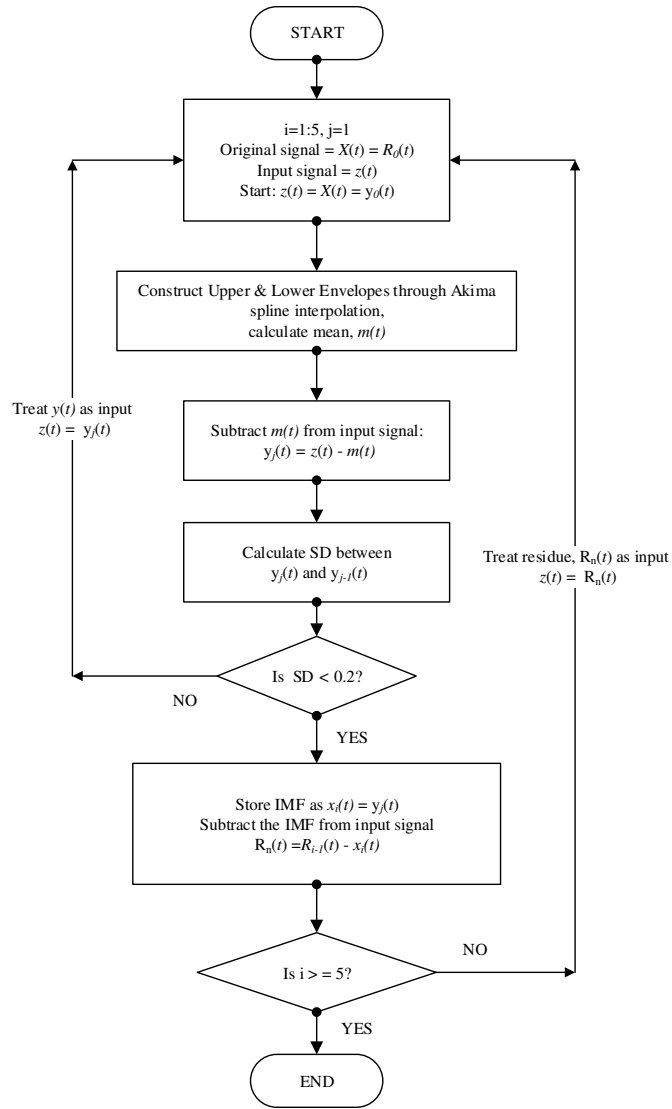


Fig. 7: Flowchart of Enhanced EMD Algorithm, FastEMD

Hence, the clean EEG sources of $S_x(t)$ and $S_y(t)$ can be estimated by taking

the weighted de-mixing matrix, A onto the observed EEG signals:

$$A = W^{-1} \quad (8)$$

$$S_x(t) = Ax(t) \quad (9)$$

$$S_y(t) = By(t) \quad (10)$$

The source signals, which are considered as the canonical variates $u(t)$ and $v(t)$ are obtained through linear combinations between the de-mixing matrices and mean removed observed EEG variables, $\hat{x}(t)$ and $\hat{y}(t)$, where n is the number of EEG sample in one channel and p is the number of channels of the EEG recording:

$$\begin{aligned} u_1 &= a_{11}\hat{x}_1 + a_{12}\hat{x}_2 + \dots + a_{1p}\hat{x}_p \\ u_2 &= a_{21}\hat{x}_1 + a_{22}\hat{x}_2 + \dots + a_{2p}\hat{x}_p \\ u_n &= a_{n1}\hat{x}_1 + a_{n2}\hat{x}_2 + \dots + a_{np}\hat{x}_p \\ v_1 &= b_{11}\hat{y}_1 + b_{12}\hat{y}_2 + \dots + b_{1p}\hat{y}_p \\ v_2 &= b_{21}\hat{y}_1 + b_{22}\hat{y}_2 + \dots + b_{2p}\hat{y}_p \\ v_n &= b_{n1}\hat{y}_1 + b_{n2}\hat{y}_2 + \dots + b_{np}\hat{y}_p \end{aligned} \quad (11)$$

which can be simplified as:

$$\begin{aligned} U &= A^T \hat{X} \\ V &= B^T \hat{Y} \end{aligned} \quad (12)$$

The purpose of CCA is finding the de-mixing matrices A and B such that the correlation, ρ between U and V , is maximized, or as large as possible. For example, the de-mixing matrices $a_1 = [a_{11}, a_{12}, \dots, a_{1p}]^T$ and $b_1 = [b_{11}, b_{12}, \dots, b_{1p}]^T$ are computed such that the coefficient of canonical correlation between the first pair of canonical variates u_1 and v_1 is maximized:

$$\rho_1 = \text{corr}(u_1, v_1) \quad (13)$$

where,

$$\begin{aligned} u_1 &= a_1^T \hat{x} \\ v_1 &= b_1^T \hat{y} \end{aligned} \quad (14)$$

The second and following pairs of canonical variates are computed in a similar way, provided that the second pair of canonical variates are uncorrelated with the first pair and other pairs of canonical variates. This procedure is repeated until enough canonical variate pairs are obtained. CCA was initially proposed in [30] by Hotelling. In EEG’s artifact removal, CCA was employed in several works to remove muscle and ocular artifacts. CCA is implemented by De Clercq et al. [14] to remove muscle artifacts from the EEG signal, followed by Hallez et al. in [31] with CCA and the blind source separation approach. Later, Zhao et al. [32] used the Wavelet in combination with CCA to remove ocular artifacts from EEG. Sweeney et al. [18] then use the Ensemble EMD with CCA to remove artifact from the EEG signal. On the other hand, M.Soomro et al. [15] has used the CCA to the entire signal with conventional EMD for removal of eyeblink artifacts in a short length of EEG signal. In this work, CCA is applied in windows to obtain canonical components and used with the combination of enhanced EMD for eyeblink artifact removal from real EEG signals of long durations.

2.3.2. Application of Windowed CCA for Eyeblink Artifact Removal

A sliding window with the length of the eyeblink artifact template is moved along the EEG signal and each window is cross-correlated with the eyeblink artifact template extracted, as in Eq. (15):

$$\rho(X, X_{EB}) = \frac{\sum_{t=1}^N X(t)X_{EB}(t)}{\sqrt{\sum_{t=1}^N X^2(t)}\sqrt{\sum_{t=1}^N X_{EB}^2(t)}} \quad (15)$$

where N represents the length of the window, $X(t)$ represents the contaminated EEG signal, and $X_{EB}(t)$ represents the eyeblink artifact template extracted from FastEMD.

Windows that exhibit high similarity scores with the eyeblink artifact template are subjected to CCA. CCA estimates the canonical components that maximize temporal correlation within the specified window. The most pertinent artifactual canonical components, U , usually the first row of the canonical components are forced to become zero in order for it to behave non-artifactual.

The artifact-free canonical components are termed as U_{clean} . Then, clean EEG segment is reconstructed by taking the inverse of the de-mixing matrix, A_x into the non-artifactual source, U_{clean} :

$$x(t)_{\text{clean}} = A^{-1}U_{\text{clean}}(t) \quad (16)$$

Fig. 8 depicts the overall block diagram of the proposed method:

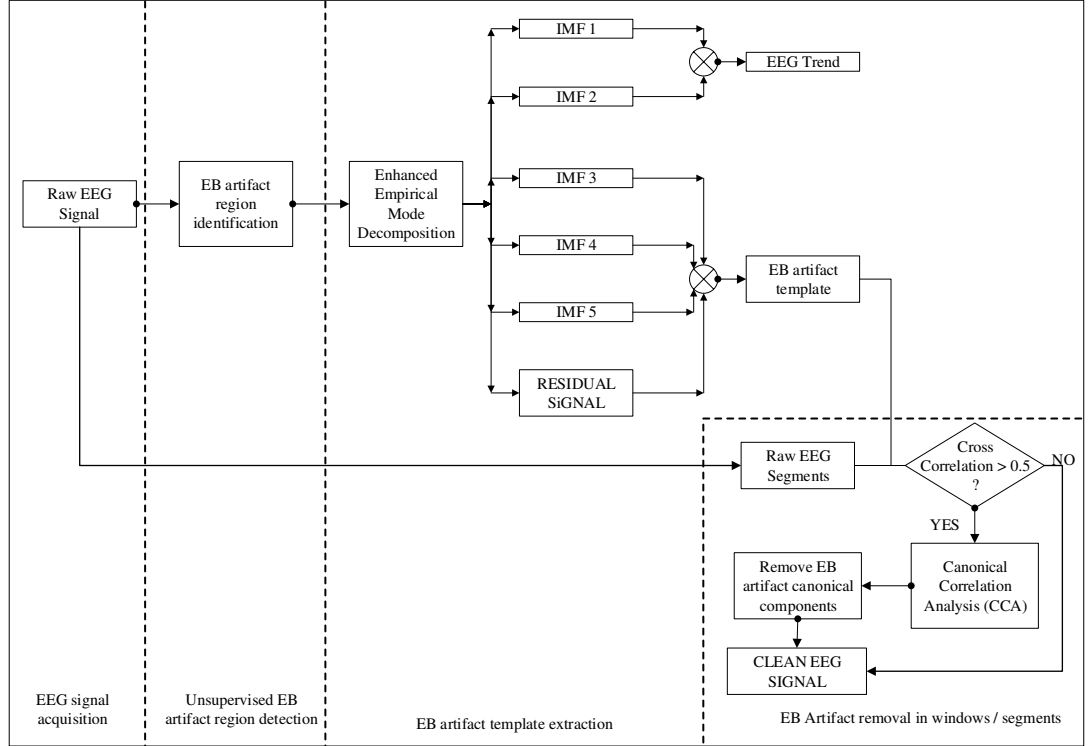


Fig. 8: Overall Block Diagram of the Proposed Algorithm, FastEMD-CCA

2.4. EEG Recording/Simulation and Analysis

2.4.1. Synthetic Signals

Synthetic eyeblink and EEG signals are simulated for validation purpose in MATLAB 2018b. Synthetic eyeblink artifacts, $Z(t)$ can be simulated through exponential functions with different amplitudes as stated in [29]:

$$Z(t) = 10e^{-(10t-10)^2} + 10e^{-(10t-30)^2} + 8e^{-(10t-45)^2} + 7e^{-(10t-70)^2} \quad (17)$$

On the other hand, a synthetic EEG signal can be generated through pink noise, $Y(t)$ for a duration of 10 seconds, 2560 samples at a sampling frequency of 256 Hz. EEG and eyeblink artifact models simulated through pink noise and exponential function are shown in Fig. 9(a) and 9(b) respectively. Both synthetic EEG signal and eyeblink artifact are mixed to acquire a set of synthetically contaminated EEG signal, $X(t)$ as in Fig. 9(c).

$$X(t) = Z(t) + Y(t) \quad (18)$$

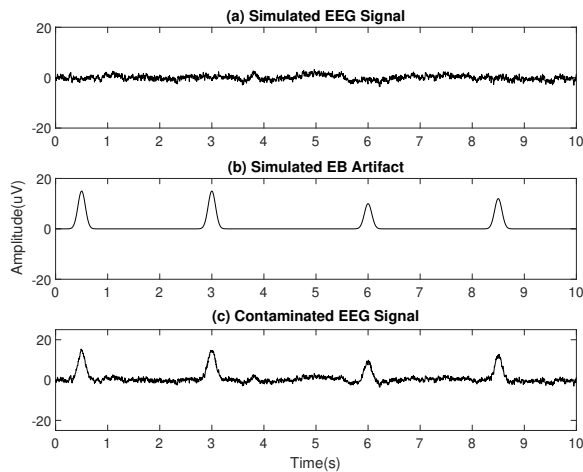


Fig. 9: (a) Synthetic EEG Signal, (b) Synthetic Eyeblink Artifact, (c) Contaminated EEG Signal

2.4.2. Real Signals

EEG data sets that were used in this paper were collected at Hitachi, Hatayoma site in Japan. EEG data from volunteers were obtained according to the regulations of the internal review board on Central Research Laboratory, Hitachi, Ltd., following receipt of written informed consent. The approval number is 20131021-0138. These EEG signals have been primarily collected to conduct a study on mental stress. Since all recorded signals were contaminated by eyeblink artifacts, we have re-use these data sets to achieve the goal of this work. These

EEG signals are recorded following the 10-20 international standardization with free electrodes placed on the scalp. The EEG signals were collected from 10 participants with 6 recordings from each participant, resulting in 60 EEG data sets. The participants are aged between 30 and 55 years. All recorded signals are of different durations, which were recorded at a sampling rate of 256 Hz.

2.5. Performance Evaluation

Any artifact removal algorithm is reflected as efficacious and successful depending on two measures. The first and most important one is how well an algorithm is able to remove the artifacts, and the second one is how well an artifact removal algorithm is able to preserve neural information contained in an EEG signal after artifact removal. On another note, the online eyeblink artifact removal capability can be interpreted through processing time taken by the algorithm. This is to evaluate the ability of the algorithm in pursuance of online processing, whether it can achieve instantaneous artifact removal without loss of neural information.

However, evaluating the performance of any algorithms in identifying and discarding artifacts is challenging in the absence of ground truths. Hence, the eyeblink artifacts and EEG signals are artificially generated as discussed in section 2.4.1. These artificial signals serve as ground truths in carrying out the performance evaluation, before applying the enhanced algorithm to real sets of EEG signals. In real EEG signal recordings, the EOG electrodes that capture eyeblinks are not recorded for convenience purposes. Additionally, there are no training data with blinking recorded so that the algorithm is fully automatic. Since EOG is not recorded, validation, if the eyeblink artifacts are removed turns out to be difficult. Thus, an expert's advice is sought to substantiate if the algorithm is able to remove eyeblink artifacts effectively through visual manual inspection (VMI).

2.5.1. Compared Approaches and Evaluation Criteria

The proposed algorithm, FastEMD-CCA is compared with two existing techniques or algorithms. Evaluation on the approaches are performed in MATLAB 2018b on Windows 7 Professional(64-bit OS, 4GB RAM).

FastEMD-CCA and Wavelet Transform

The developed algorithm, FastEMD-CCA is compared with Wavelet Transform, to evaluate the performance exhibited by these algorithms on the synthetically contaminated EEG signal, in Eq. (18). The synthetic EEG signal and the eyeblink artifacts are simulated for 100 trials for reliability purposes, and the results are averaged. Wavelet is chosen as it has been extensively used for eyeblink artifact removal in EEG [12, 33, 34]. The FastEMD-CCA works as discussed in sections 2.1, 2.2 and 2.3. For Wavelet Transform, the sym9 mother wavelet from the Symlets family is chosen as it was suggested as resembling EEG signals the most and would be the most compatible one for de-noising purposes by Al-Qazzaz et al. [35]. SWT is applied with soft thresholding on the entire contaminated EEG signal to obtain wavelet coefficients. Larger coefficients are assumed to correspond to the artifact and smaller coefficients are assumed to correspond to EEG. The inverse of SWT, ISWT is then applied on the coefficients corresponding to EEG and artifact to reconstruct the clean EEG signal and the eyeblink artifact respectively.

The performance of these algorithms in retaining the neural information in an EEG signal is quantitatively assessed. Reconstructed EEG signals after artifacts have been removed via these algorithms are validated against synthetically generated EEG signals as ground truths. Ideally, reconstructed EEG signals should remain intact after artifacts have been removed. The algorithms are evaluated in terms of correlations coefficient (CC), root means square error (RMSE) and signal to noise ratio (SNR), in the time domain. Each of the performance criteria is expressed as confidence intervals for 95% of confidence level. CC_{eeg} measures the similarity between synthetically generated EEG signals with its corresponding reconstructed EEG signals after artifact correction,

while CC_{eb} estimates the resemblance of removed eyeblink artifacts compared to synthetic eyeblink artifacts. RMSE measures the removal and reconstruction error for eyeblink and EEG signals respectively. The RMSE is calculated by finding the difference between synthetically generated eyeblink artifacts with removed eyeblink artifacts, $RMSE_{\text{eb}}$ and synthetically generated EEG signals with reconstructed signals, $RMSE_{\text{eeg}}$ after processing with the suggested techniques. The SNR is used in this analysis to determine the ratio of signal to artifact that remains after eyeblink artifact has been removed from the contaminated EEG signal. The SNR ratio is calculated before and after eyeblink artifact removal, using Eq. (23) and (24).

$$CC_{\text{eeg}} = \frac{\text{cov}(Y, Y_1)}{\text{std}(Y) * \text{std}(Y_1)} \quad (19)$$

$$CC_{\text{eb}} = \frac{\text{cov}(Z, Z_1)}{\text{std}(Z) * \text{std}(Z_1)} \quad (20)$$

$$RMSE_{\text{eeg}} = \sqrt{\frac{\sum_{t=1}^n (Y(t) - Y_1(t))^2}{n}} \quad (21)$$

$$RMSE_{\text{eb}} = \sqrt{\frac{\sum_{t=1}^n (Z(t) - Z_1(t))^2}{n}} \quad (22)$$

$$\text{SNR}_{\text{before}} = 10 \log \left[\frac{\text{std}(Y)}{\text{std}(Y - X)} \right] \quad (23)$$

$$\text{SNR}_{\text{after}} = 10 \log \left[\frac{\text{std}(Y)}{\text{std}(Y - Y_1)} \right] \quad (24)$$

where $X(t)$ represents the synthetically contaminated EEG signals, $Y(t)$ refers to the simulated/synthetic EEG signals generated using pink noise, $Y_1(t)$ corresponds to the reconstructed EEG signals which are free from artifacts, $Z(t)$ refers to the synthetic eyeblink artifact and $Z_1(t)$ corresponds to the extracted

eyeblick artifact. From the performance metrics, 95% of confidence interval has been estimated so that the probability of the performance is repetitive over 95% of the time, if the evaluation to be repeated multiple times in another time frame.

FastEMD-CCA and FORCe

Real EEG signals illustrated in section 2.4.2 were used to evaluate the proposed, FastEMD-CCA and the state-of-the-art, FORCe algorithms. The outcomes are then averaged for these 60 sets of EEG signals. In MATLAB, the EEG recordings are imported into the workspace and processed automatically to remove the eyeblink artifacts in windows, with each window is minimally 1s in length for both FastEMD-CCA and FORCe. The FastEMD-CCA algorithm operates as discussed in sections 2.1, 2.2 and 2.3. The FORCe algorithm first applies wavelet decomposition on each channel of an EEG signal. Resulting approximation coefficients attained through wavelet are subjected to ICA to get independent components, ICs. Next, the artifactual ICs are identified through several threshold criteria, where ICs exceeding certain threshold values are classified as eyeblink and electrocardiogram artifacts respectively, and thus removed. The inverse of ICA is performed to estimate a set of cleaned approximation coefficients. Then, soft thresholding is applied to resulting approximation coefficients from ICA and detail coefficients acquired through wavelet to suppress/remove EMG artifacts. Finally, a clean EEG signal is reconstructed.

Since the ground truth are not available for real EEG data sets, the efficacy of both algorithms in identifying and removing eyeblink artifacts, while preserving the artifact-free EEG segments are verified with the help of an expert, Neuroscientist Dr. Tahamina, through VMI. The evaluation criteria are derived from various measures of the binary prediction [36, 37], thus determining the accuracy, sensitivity, specificity and error rate of the algorithms.

3. Results and Discussions

3.1. Evaluation on Synthetic Signals

The proposed algorithm, FastEMD-CCA is compared with Wavelet Transform as elaborated in section 2.4.1, to evaluate the performance exhibited by these algorithms on synthetically generated EEG signals. Fig. 10(a) - 10(c) show the reconstructed EEG signal and eyeblink artifact through FastEMD-CCA. Fig. 11(a) - 11(c) show the reconstructed EEG signal and eyeblink artifact through SWT.

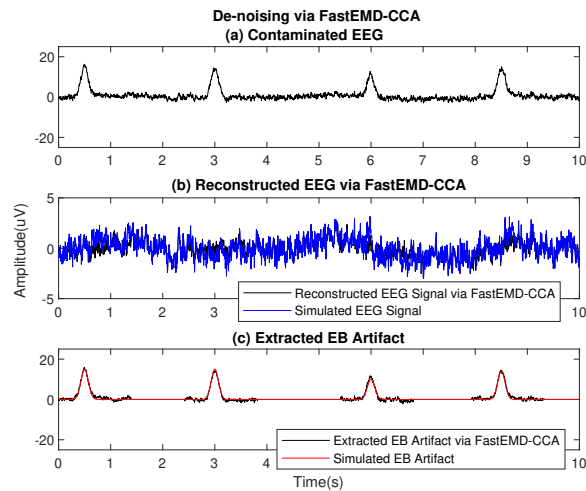


Fig. 10: (a) Mixed EEG and Eyeblink Signal, (b) Reconstructed EEG Signal, (c) Extracted Eyeblink Artifact

The performance metrics obtained for FastEMD-CCA and Wavelet Transform, applied on synthetically generated and contaminated EEG signals are tabulated in Table 1.

3.1.1. Discussion

The algorithms are evaluated on 100 trials of synthetically contaminated signals to ensure the performance exhibited by the algorithms are reliable and repetitive. The confidence interval for 95% of confidence level is determined for

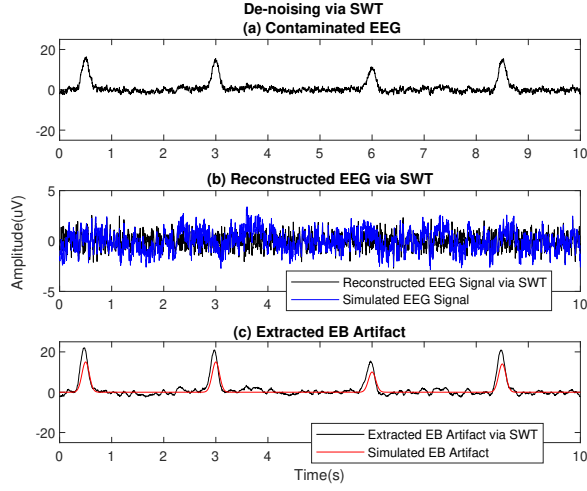


Fig. 11: (a) Mixed EEG and Eyeblink Signal, (b) Reconstructed EEG Signal, (c) Extracted Eyeblink Artifact

Table 1: Performance Metrics of Synthetic Signals

Techniques	Wavelet (SWT)		FastEMD-CCA	
	mean \pm std ($\mu \pm \sigma$)	95% CI	mean \pm std ($\mu \pm \sigma$)	95% CI
<i>CCeeg</i>	0.6479 \pm 0.0332	0.6413 to 0.6545	0.7478 \pm 0.0687	0.7341 to 0.7614
<i>CCeb</i>	0.9272 \pm 0.0065	0.9259 to 0.9285	0.9754 \pm 0.0055	0.9743 to 0.9765
<i>RMSEeeg</i>	0.7641 \pm 0.0272	0.7587 to 0.7695	0.6580 \pm 0.0776	0.6426 to 0.6734
<i>RMSEeb</i>	1.9562 \pm 0.0894	1.9385 to 1.9740	0.6580 \pm 0.0776	0.6426 to 0.6734
<i>SNRafter (dB)</i>	2.6967 \pm 0.3560	2.6260 to 2.7673	4.2845 \pm 1.2200	4.0424 to 4.5265
<i>SNRbefore (dB)</i>	-10.6594 \pm 0.00	-10.6594	-10.6594 \pm 0.00	-10.6594
<i>Time (s)</i>	0.0226 \pm 0.0065	0.0213 to 0.0239	3.2489 \pm 3.9818	2.4584 to 4.0386

each of the performance metrics. The 95% confidence level is chosen so that the estimation of results are statistically sound. CC value normally lies between -1 and 1, in which a value approaching 1 indicates a higher correlation or similarity. RMSE value that approaches zero signifies a more precise and accurate signal reconstruction, relative to the synthetic signals. The SNR measures the scale of eyeblink artifacts that have been removed from the noisy EEG signal and the degree of neural signal preservation. The effectiveness of the evaluated algorithms in preserving the underlying neural information in an EEG signal

can be deduced through CC value that approaches near 1, RMSE close to 0 and higher SNR value. In this analysis between Wavelet and the proposed technique, FastEMD-CCA has produced higher CC values on average compared to SWT, 0.7478 in reconstructing the EEG signal and 0.9754 in extracting out the eyeblink artifact. The error produced by FastEMD-CCA is 14% percent lower than the error produced by SWT in reconstructing the EEG signal. While in extracting out the eyeblink artifact, FastEMD-CCA has produced an error of 66% lower than SWT. This indicates that the FastEMD-CCA algorithm is able to remove eyeblink artifact components appropriately from the contaminated EEG signal in comparison with SWT. From Table 1, FastEMD-CCA yields very high SNR, close to 4 dB on average from -10dB before artifact correction, which denotes a higher ratio of neural information has been preserved. Alternatively, SWT produced nearly 2dB of SNR on average from -10dB before artifact elimination. This shows that the FastEMD-CCA is a better choice in removing eyeblink artifacts, and at the same time, it is able to preserve underlying EEG components better, by not introducing much distortion to the neural signal. In terms of computation time, the SWT is way faster than the FastEMD-CCA. It has to be emphasized here that SWT removes artifacts only from a single channel EEG signal, hence faster computation time, while FastEMD-CCA performs the artifact elimination from a multichannel EEG signal. Moreover, SWT is applied to the entire signal for processing which is not applicable for online applications, while the FastEMD-CCA algorithm process the EEG signals in windows. SWT also relies on manual selection of appropriate mother wavelet, comprises sine and cosine functions, which may not represent a basis function for non-stationary biomedical signals. Selecting an inappropriate mother wavelet could lead to inaccuracy in reconstructing artifact-free EEG signals. Furthermore, the accuracy of SWT is also sensitive to the selection of thresholding function which could have an effect on preserving or discarding the neural information in an EEG signal. Considering the performance shown by FastEMD-CCA by means of accuracy in removing artifacts, it's used for evaluation in removing artifacts in real EEG signals.

3.2. Evaluation on Real EEG Signals

Results in Table 2 were obtained through offline analysis performed on the artifact removed EEG signals in an online manner through the proposed technique, FastEMD-CCA and the state-of-the-art algorithm, FORCE. Fig. 12 and 13 shows an example of an entire EEG signal, reconstructed using FORCE algorithm and the proposed algorithm, FastEMD-CCA respectively. Fig. 14 and 15 show a short portion of the EEG signal, reconstructed using FORCE algorithm and the proposed algorithm, FastEMD-CCA respectively.

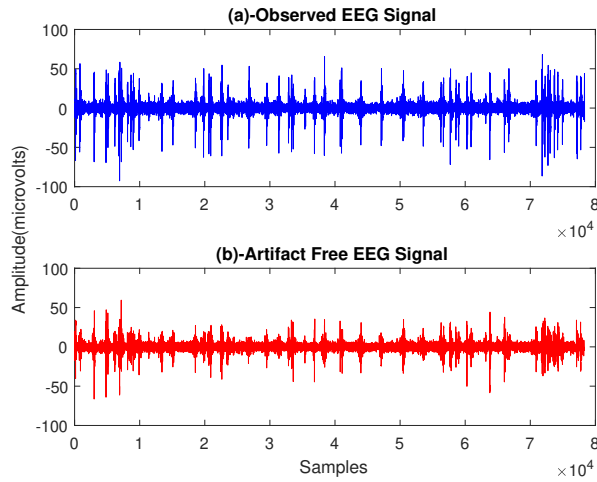


Fig. 12: Entire EEG Signal-Reconstructed through FORCE

The average of accuracy, sensitivity, specificity, error rate and computation time for FastEMD-CCA and FORCE are tabulated in Table 2. The representation of error, accuracy, sensitivity, specificity and computation time for both FORCE and FastEMD-CCA are shown in Fig. 16.

3.2.1. Discussion

Accuracy is a measurement of correct detection of eyeblink artifacts by the algorithms, thus removing them, and also how well the algorithms could retain the artifact-free EEG segments after artifact correction is performed. The proposed algorithm has achieved an average of 97.9% accuracy compared to 91.7%

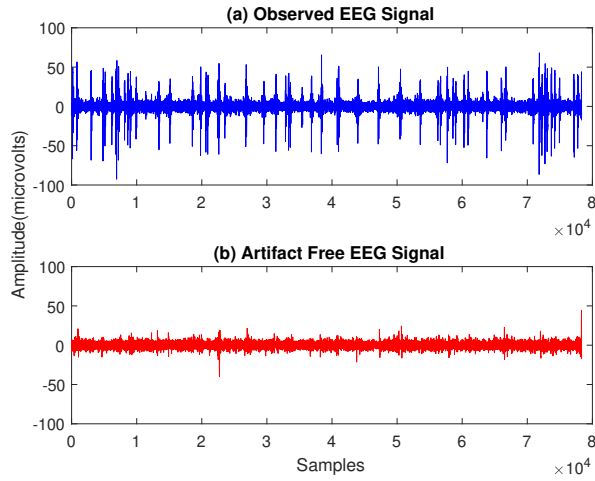


Fig. 13: Entire EEG Signal-Reconstructed through FastEMD-CCA

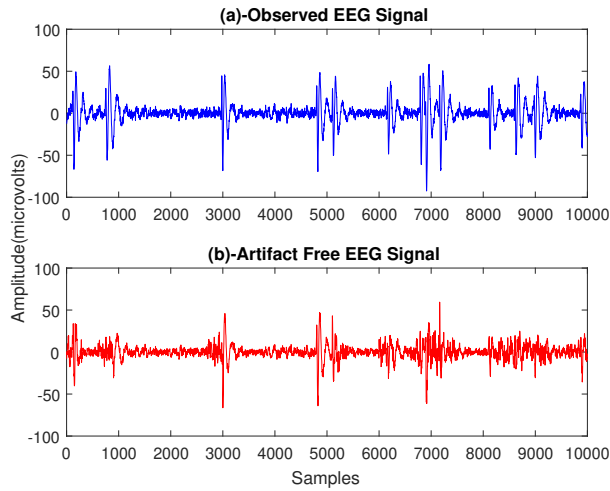


Fig. 14: A Portion of the EEG Signal-Reconstructed through FORCe

by FORCe. The higher accuracy level of the proposed algorithm, FastED-CCA over FORCe by 6.2% clearly reflects the effectiveness of the algorithm in correctly identifying and removing eyeblink artifacts from EEG signals in on-line applications. Contrarily, the error rate is the exact opposite of accuracy. FastEMD-CCA produced an average error rate of 2.10% while FORCe yields

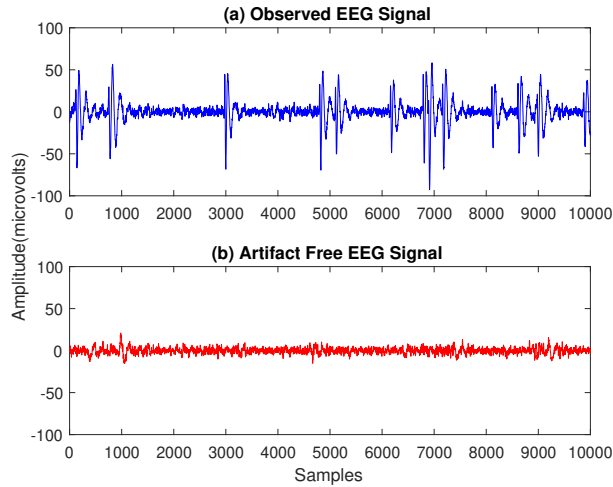


Fig. 15: A Portion of the EEG Signal-Reconstructed through FastEMD-CCA

Table 2: Performance Metrics of Real EEG Signals

Techniques	FORCe	FastEMD-CCA
Accuracy	91.70 %	97.90 %
Sensitivity	89.47 %	97.65 %
Specificity	98.65 %	99.22 %
Error	8.30 %	2.10 %
Time	85.10 s	19.73 s

8.30%. This denotes that both algorithms are still susceptible to miss out an eyeblink artifact, however, the proposed algorithm is more reliable in detecting and removing eyeblink artifacts in online applications compared to FORCe. Sensitivity, on the other hand, is a measurement of how sensitive the algorithms are in detecting and removing the eyeblink artifacts in comparison with the actual number of observed eyeblink artifacts. The results indicate the proposed algorithm, FastEMD-CCA has achieved 97.65% of sensitivity, 8.18% higher than that of the FORCe algorithm. This shows that FastEMD-CCA could identify and remove eyeblink artifacts relatively better than FORCe could. The sensitivity of FORCe in identifying and removing the artifacts is 89.47 %. This

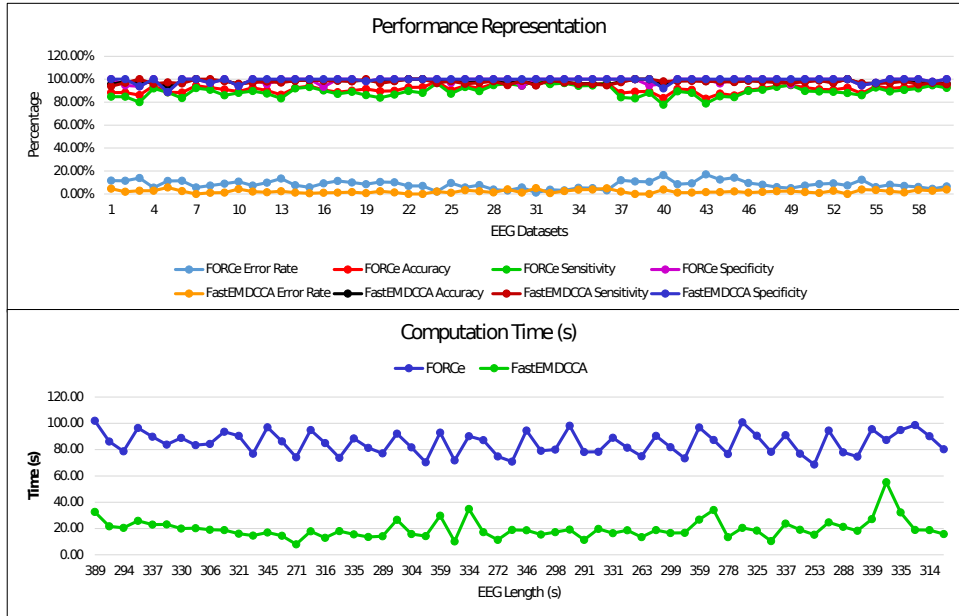


Fig. 16: Graphical Representation of the Performance

lower percentage level of sensitivity could have been due to the inability of the algorithm in identifying some of the artifact events. The identification of artifact related ICs in FORCe during ICA application on the wavelet coefficients are dependent on manually adjusted threshold values, which classifies or make a binary decision whether an IC is artifactual. So, having manually adjusted fix thresholds may lead to detection errors, thereby not removing some of the artifacts. On a separate note, the performance of the algorithms in retaining the neural information of an EEG signal is evaluated through specificity. Specificity is the ratio of undistorted artifact-free EEG segments before and after artifact elimination is performed. The ideal expectation is to have these portions undistorted after the artifacts have been removed. FastEMD-CCA and FORCe records an average specificity of 99.22% and 98.65% respectively, which signifies that both algorithms doesn't introduce much distortion to the neural information of the EEG signals under evaluation. From the comparison, it is clear that FastEMD-CCA has achieved better performance than FORCe on the

same set of EEG signals. The average computation time FastEMD-CCA took to remove eyeblink artifacts from all 14 channels of these 60 EEG data-sets with an average signal length of 312s (5 minutes) is 19.73 seconds, while FORCE took 85.10 seconds. The computation time of FastEMD-CCA is at least 4 times faster than that of FORCE.

The results have pointed out that the proposed algorithm, FastEMD-CCA is highly accurate in removing eyeblink artifacts, proved by accuracy, error rate and sensitivity measurement. It is also capable of retaining underlying EEG data in uncontaminated EEG portions which were indicated by the specificity percentage. Apart from this, the algorithm is also able to remove eyeblink artifacts when the eyeblink artifacts are in continuous sequence as highlighted in Fig. 17. The computation time of the algorithm is low as well, with an average of 63 milliseconds processing time to remove artifacts from 1-second length of EEG signal with 14 channels (256 samples x 14 EEG channels). This makes it a feasible solution for applications requiring online removal of eyeblink artifacts, with very low distortion to the neural signal.

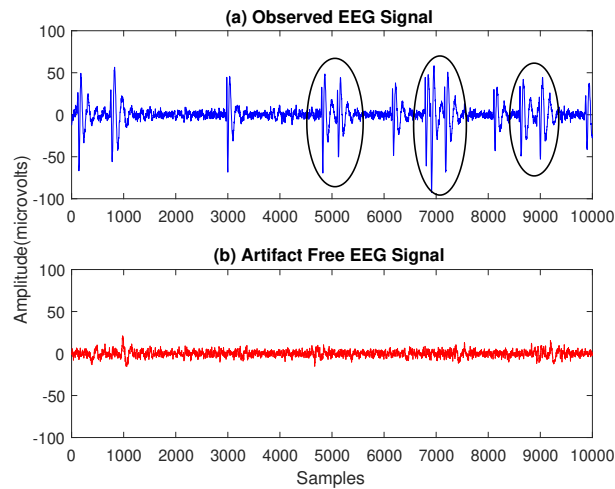


Fig. 17: Continuous Eyeblink Artifacts are Detected and Removed

4. Conclusion

This paper has discussed an efficacious algorithm that incorporates unsupervised artifact detection algorithm, enhanced-EMD, and windowed-CCA to automatically identify and eliminate eyeblink artifacts from EEG signals without the need to have an EOG channel as an artifact reference. The first portion of the algorithm identifies the eyeblink artifacts without human intervention, thus it can be also useful for other applications to utilize the eyeblink pattern/template. Apart from artifact removal, applications, where eyeblink patterns may be useful, are the driver drowsiness detection through eyeblink pattern, stress level detection using eyeblink pattern/rate and for home applications such as home light system triggering using eye blinking. The enhanced version of EMD is developed mainly to improve its processing time as conventional EMD is relatively slow due to its iterative nature. CCA is then performed in a windowed manner to characterize an online scenario. The algorithm as a whole is an unsupervised and a fast approach that performs well in identifying and removing eyeblink artifacts while preserving the underlying neural information as revealed by the results. The computation environment for eyeblink artifact removal in EEG plays a vital role in online applications. Although eyeblink artifact removal is achievable using various methods, a medium or tool that supports and aid in speeding up the eyeblink artifact removal process has not been sufficiently studied. Currently, MATLAB is the most preferred tool used for research purposes, but for online applications MATLAB may not be a feasible platform. Hence, future work will be in the direction of executing the algorithm, FastEMD-CCA in an inexpensive computing environment such as in C++ and GPU based platform as to support online applications.

Acknowledgment

The authors would like to thank the Ministry of Education, Malaysia for supporting this research through the Fundamental Research Grant Scheme, FRGS

(FRGS/2/2014/TK03/UTP/02/1) and the Higher Institution Centre of Excellence (HICoE) Scheme.

References

- [1] J. A. Urigüen, B. Garcia-Zapirain, EEG Artifact Removal - State of the Art and Guidelines, *Journal of Neural Engineering* 12 (3) (2015) 031001.
- [2] G. H. Klem, H. O. Lüders, H. Jasper, C. Elger, et al., The Ten-twenty Electrode System of the International Federation, *Electroencephalographic Clinical Neurophysiology* 52 (3) (1999) 3–6.
- [3] S. Sanei, J. A. Chambers, *EEG Signal Processing*, John Wiley & Sons, 2013.
- [4] J. Minguiñon, M. A. Lopez-Gordo, F. Pelayo, Trends in EEG-BCI for Daily-life: Requirements for Artifact Removal, *Biomedical Signal Processing and Control* 31 (2017) 407–418.
- [5] G. Gratton, M. G. Coles, E. Donchin, A New Method for Off-line Removal of Ocular Artifact, *Electroencephalography and Clinical neurophysiology* 55 (4) (1983) 468–484.
- [6] J. L. Kenemans, P. Molenaar, M. N. Verbaten, J. L. Slangen, Removal of the Ocular Artifact from the EEG: A Comparison of Time and Frequency Domain Methods with Simulated and Real Data, *Psychophysiology* 28 (1) (1991) 114–121.
- [7] J. Woestenburg, M. Verbaten, J. Slangen, The Removal of the Eye-movement Artifact from the EEG by Regression Analysis in the Frequency Domain, *Biological Psychology* 16 (1-2) (1983) 127–147.
- [8] P. Berg, M. Scherg, Dipole Modelling of Eye Activity and its Application to the Removal of Eye Artefacts from the EEG and MEG, *Clinical Physics and Physiological Measurement* 12 (A) (1991) 49.

- [9] T. D. Lagerlund, F. W. Sharbrough, N. E. Busacker, Spatial Filtering of Multichannel Electroencephalographic Recordings through Principal Component Analysis by Singular Value Decomposition, *Journal of Clinical Neurophysiology* 14 (1) (1997) 73–82.
- [10] T.-P. Jung, C. Humphries, T.-W. Lee, S. Makeig, M. J. McKeown, V. Iragui, T. J. Sejnowski, Extended ICA Removes Artifacts from Electroencephalographic Recordings, in: *Advances in Neural Information Processing Systems*, 1998, pp. 894–900.
- [11] R. Vigário, J. Sarela, V. Jousmiki, M. Hamalainen, E. Oja, Independent Component Approach to the Analysis of EEG and MEG Recordings, *IEEE Transactions on Biomedical Engineering* 47 (5) (2000) 589–593.
- [12] V. Krishnaveni, S. Jayaraman, S. Aravind, V. Hariharasudhan, K. Ramadoss, Automatic Identification and Removal of Ocular Artifacts from EEG Using Wavelet Transform, *Measurement Science Review* 6 (4) (2006) 45–57.
- [13] Q. Zhao, B. Hu, Y. Shi, Y. Li, P. Moore, M. Sun, H. Peng, Automatic Identification and Removal of Ocular Artifacts in EEG Improved Adaptive Predictor Filtering for Portable Applications, *IEEE Transactions on Nanobioscience* 13 (2) (2014) 109–117.
- [14] W. De Clercq, A. Vergult, B. Vanrumste, W. Van Paesschen, S. Van Huffel, Canonical Correlation Analysis Applied to Remove Muscle Artifacts from the Electroencephalogram, *IEEE Transactions on Biomedical Engineering* 53 (12) (2006) 2583–2587.
- [15] M. H. Soomro, N. Badruddin, M. Z. Yusoff, M. A. Jatoi, Automatic Eyeblink Artifact Removal Method Based on EMD-CCA, in: *ICME International Conference on Complex Medical Engineering*, IEEE, 2013, pp. 186–190.
- [16] M. Shahbakhti, V. Khalili, G. Kamaee, Removal of Blink from EEG by

- Empirical Mode Decomposition (EMD), in: Biomedical Engineering International Conference (BMEiCON), IEEE, 2012, pp. 1–5.
- [17] B. Raghavendra, D. N. Dutt, Correction of Ocular Artifacts in EEG Recordings Using Empirical Mode Decomposition, National Conference on Communication.
- [18] K. T. Sweeney, S. F. McLoone, T. E. Ward, The Use of Ensemble Empirical Mode Decomposition with Canonical Correlation Analysis as a Novel Artifact Removal Technique, IEEE Transactions on Biomedical Engineering 60 (1) (2013) 97–105.
- [19] N. E. Huang, Z. Shen, S. R. Long, M. C. Wu, H. H. Shih, Q. Zheng, N.-C. Yen, C. C. Tung, H. H. Liu, The Empirical Mode Decomposition and the Hilbert Spectrum for Nonlinear and Non-stationary Time Series Analysis, in: Proceedings of the Royal Society of London : A Mathematical, Physical and Engineering Sciences, Vol. 454, The Royal Society, 1998, pp. 903–995.
- [20] D. Labate, F. La Foresta, G. Occhiuto, F. C. Morabito, A. Lay-Ekuakille, P. Vergallo, Empirical Mode Decomposition vs. Wavelet Decomposition for the Extraction of Respiratory Signal from Single-channel ECG: A Comparison, IEEE Sensors Journal 13 (7) (2013) 2666–2674.
- [21] B. Nouredin, P. D. Lawrence, G. E. Birch, Online Removal of Eye Movement and Blink EEG Artifacts Using a High-speed Eye Tracker, IEEE Transactions on Biomedical Engineering 59 (8) (2011) 2103–2110.
- [22] M. K. Islam, A. Rastegarnia, Z. Yang, Methods for Artifact Detection and Removal from Scalp EEG: A Review, Neurophysiologie Clinique/Clinical Neurophysiology 46 (4-5) (2016) 287–305.
- [23] S. Çınar, N. Acır, A Novel System for Automatic Removal of Ocular Artefacts in EEG by Using Outlier Detection Methods and Independent Component Analysis, Expert Systems with Applications 68 (2017) 36–44.

- [24] V. Lawhern, W. D. Hairston, K. McDowell, M. Westerfield, K. Robbins, Detection and Classification of Subject-generated Artifacts in EEG Signals Using Autoregressive Models, *Journal of Neuroscience Methods* 208 (2) (2012) 181–189.
- [25] H.-A. T. Nguyen, J. Musson, F. Li, W. Wang, G. Zhang, R. Xu, C. Richey, T. Schnell, F. D. McKenzie, J. Li, EOG Artifact Removal Using a Wavelet Neural Network, *Neurocomputing* 97 (2012) 374–389.
- [26] I. Daly, R. Scherer, M. Billinger, G. Müller-Putz, FORCe: Fully Online and Automated Artifact Removal for Brain Computer Interfacing, *IEEE Transactions on Neural Systems and Rehabilitation Engineering* 23 (5) (2015) 725–736.
- [27] L. Pion-Tonachini, S.-H. Hsu, C.-Y. Chang, T.-P. Jung, S. Makeig, Online Automatic Artifact Rejection Using the Real-time EEG Source-mapping Toolbox (REST), in: 2018 40th Annual International Conference of the IEEE Engineering in Medicine and Biology Society (EMBC), IEEE, 2018, pp. 106–109.
- [28] A. Egambaram, N. Badruddin, V. S. Asirvadam, E. Fauvet, C. Stolz, T. Begum, Unsupervised Eye Blink Artifact Identification in Electroencephalogram, in: TENCON 2018-2018 IEEE Region 10 Conference, IEEE, 2018, pp. 2148–2152.
- [29] A. Egambaram, N. Badruddin, V. S. Asirvadam, T. Begum, Comparison of Envelope Interpolation Techniques in Empirical Mode Decomposition (EMD) for Eyeblick Artifact Removal from EEG, in: IEEE EMBS Conference on Biomedical Engineering and Sciences (IECBES), IEEE, 2016, pp. 590–595.
- [30] H. Hotelling, Relations Between Two Sets of Variates, *Biometrika* 28 (3/4) (1936) 321–377.

- [31] H. Hallez, M. De Vos, B. Vanrumste, P. Van Hese, S. Asseconi, K. Van Laere, P. Dupont, W. Van Paesschen, S. Van Huffel, I. Lemahieu, Removing Muscle and Eye Artifacts Using Blind Source Separation Techniques in Ictal EEG Source Imaging, *Clinical Neurophysiology* 120 (7) (2009) 1262–1272.
- [32] C. Zhao, T. Qiu, An Automatic Ocular Artifacts Removal Method Based on Wavelet-enhanced Canonical Correlation Analysis, in: Annual International Conference of the IEEE Engineering in Medicine and Biology Society, EMBC, IEEE, 2011, pp. 4191–4194.
- [33] P. S. Kumar, R. Arumuganathan, K. Sivakumar, C. Vimal, Removal of Ocular Artifacts in the EEG through Wavelet Transform without Using an EOG Reference Channel, *Int. J. Open Problems Compt. Math* 1 (3) (2008) 188–200.
- [34] S. Khatun, R. Mahajan, B. I. Morshed, Comparative Study of Wavelet-based Unsupervised Ocular Artifact Removal Techniques for Single-channel EEG Data, *IEEE Journal of Translational Engineering in Health and Medicine* 4 (2016) 1–8.
- [35] N. K. Al-Qazzaz, S. Hamid Bin Mohd Ali, S. A. Ahmad, M. S. Islam, J. Escudero, Selection of Mother Wavelet Functions for Multi-channel EEG Signal Analysis During a Working Memory Task, *Sensors* 15 (11) (2015) 29015–29035.
- [36] D. B. Stone, G. Tamburro, P. Fiedler, J. Haueisen, S. Comani, Automatic Removal of Physiological Artifacts in EEG: The Optimized Fingerprint Method for Sports Science Applications, *Frontiers in Human Neuroscience* 12 (2018) 96.
- [37] S. ORegan, S. Faul, W. Marnane, Automatic Detection of EEG Artefacts Arising from Head Movements Using EEG and Gyroscope Signals, *Medical Engineering & Physics* 35 (7) (2013) 867–874.